ORGANIC CHEMISTRY FRONTIERS

RESEARCH ARTICLE

View Article Online
View Journal

Cite this: DOI: 10.1039/d6qo00078a

A divergent electrochemical platform for diazene radical generation and C–N coupling reactions

Roopam Pandey, †[a] Suchismita Rath,†[a] Yashika Tyagi,[a] Shivani Jadon,[a] Tejas Prabakar,[a] Shreemad Patel,[a] Debajit Maiti[b] and Subhabrata Sen *[a]

Received 20th January 2026,
Accepted 1st March 2026

DOI: 10.1039/d6qo00078a

rsc.li/frontiers-organic

The development of sustainable methods for controlled C–N bond formation remains a central challenge in modern synthesis. Here we report an operationally simple, catalyst-free and acid/base-free electrochemical platform that enables the direct single-electron activation of N-carbazates to generate a versatile diazene-centred radical under direct current (DC) or rapid alternating polarity current (rAP). This is the first general electrochemical access to diazene radicals. The *in situ*–formed nitrogen radical engages *aryl* diazoacetates *via* radical coupling after dinitrogen extrusion (*via* blue LED), delivering a diverse library of *N*-acyl hydrazones. The same radical intermediate undergoes a Michael-type conjugate addition to *N*-aryl maleimides, affording imide-linked hydrazine derivatives, thereby establishing a rare example of radical divergence from a single electrochemically generated intermediate. The method is broadly applicable across 9 carbazate classes affording 35 products, including drug-derived motifs, and proceeds under mild conditions in the absence of external reductants or catalysts. Together, these results introduce a sustainable, redox-economical strategy for N–C bond construction and expand the synthetic utility of hydrazine radicals in electroorganic chemistry.

Introduction

Hydrazine-containing functional groups constitute a privileged class of motifs in organic synthesis, appearing in biologically active molecules, pharmaceutical agents, agrochemicals, and as key precursors to heterocycles and ligands.[1–5] Their high nucleophilicity, redox activity, and structural versatility have positioned hydrazines as indispensable building blocks in medicinal chemistry and synthetic methodology. Despite their widespread utility, however, existing approaches to hydrazine derivatives remain limited by safety, practicality, and sustainability concerns. Classical protocols often rely on hazardous hydrazine reagents, strong reductants, or multistep sequences involving protecting groups, all of which compromise atom economy and generate significant chemical waste.[6–13] Developing mild, selective, and environmentally responsible routes to hydrazine frameworks therefore remains an outstanding challenge.

In parallel, N-centered radicals have emerged as powerful and versatile intermediates capable of enabling transformations that are difficult or inaccessible through conventional two-electron chemistry.[14–18] Their capacity to mediate selective C–N bond formation, remote functionalization, and intramolecular cyclization has broadened the synthetic toolbox for constructing nitrogen-rich scaffolds of relevance to pharmaceuticals and functional materials. Recent reviews highlight that N-centered radicals can be generated from diverse precursors—including amines, amides, imides, hydrazines, and N-halogenated species—and have enabled site-selective functionalization of (hetero)arenes and sp^2 systems under photochemical or electrochemical activation.[19–22] Despite such advances, diazene-based N-centered radicals remain scarcely explored due to the instability of their precursors, competing decomposition pathways, and the need for strong oxidants or specialized photoredox catalysts. Notably, prior reports involving carbazates under oxidative or photochemical conditions have primarily focused on fragmentation pathways, carbene transfer, or two-electron processes, rather than the controlled generation and productive interception of persistent diazene-centred radicals.[23] In many cases, these approaches require transition-metal catalysts, stoichiometric oxidants, or carefully tuned photoredox systems, and often suffer from competing N–N bond cleavage or uncontrolled radical decomposition. Thus, a general and sustainable strategy for accessing these reactive intermediates would address a key limitation in nitrogen-radical chemistry.

Electroorganic synthesis has emerged as a robust platform for enabling single-electron processes in a sustainable

[a]Department of Chemistry, School of Natural Sciences, Shiv Nadar Institution of Eminence Deemed to be University, Chithera, Dadri, Gautam Buddha Nagar, UP 201314, India. E-mail: subhabrata.sen@snu.edu.in
[b]Department of Chemistry, School of Interwoven Arts and Sciences, Krea University, Sri City, Andhra Pradesh 517 646, India
† Equal contribution.

manner, offering a green alternative to chemical oxidants and reductants.[24–26] Yet within this field, the controlled electrochemical generation of diazene-centered radicals has remained underdeveloped, largely due to challenges in designing suitable precursors and managing radical reactivity under operationally simple conditions. To the best of our knowledge, a general electrochemical platform that directly oxidizes stable N-carbazates to furnish synthetically competent diazene-centred radicals without external catalysts, chemical oxidants, or acidic/basic additives—has not been established. A method capable of directly converting stable, readily available feedstocks into hydrazine radicals—without acids, bases, catalysts, or stoichiometric redox reagents—would markedly expand the landscape of N-centered radical chemistry and align with the principles of green synthesis.

Diazo compounds, particularly aryl diazoacetates, hold a distinguished place in synthesis owing to their versatility as carbene precursors.[27,28] Under photochemical excitation, they furnish singlet and triplet carbenes that mediate diverse bond constructions. Under electro-photochemical conditions, however, diazo esters can undergo single-electron reduction to generate carbene radical anions, opening new mechanistic pathways for C–H, N–H, and C=C functionalization through radical coupling processes.[29–31] Their unique redox properties therefore make diazo compounds ideal partners for engaging nitrogen-centered radicals in previously inaccessible bond-forming reactions.

N-Acyl hydrazones constitute a synthetically and pharmacologically valuable class, exhibiting broad structural tunability and diverse biological activities, including antibacterial, antihemorrhagic, and antibiotic properties (Scheme 1A).[32,33] The design of sustainable, efficient synthetic routes to *N*-acyl hydrazones is thus of significant interest for both medicinal and synthetic chemistry.

Here we report an operationally simple, catalyst-free, and acid/base-free electrochemical strategy that directly oxidizes *N*-carbazates to generate a persistent diazene-centered radical under constant-current electrolysis (DC or rAP) (Scheme 1B). In contrast to prior oxidative protocols that promote rapid N–N bond fragmentation or require photoredox mediation, the present system enables controlled radical formation under mild electrochemical conditions, thereby allowing productive interception before decomposition. This radical intermediate participates in two mechanistically distinct and synthetically valuable pathways. In the presence of aryl diazoacetates, it undergoes radical–radical anion coupling following rapid N_2 extrusion, delivering a diverse library of *N*-acyl hydrazones (Scheme 1B). Alternatively, the same diazene radical undergoes Michael-type conjugate addition to *N*-aryl maleimides to furnish imide-linked hydrazine derivatives (Scheme 1B). The ability to access two distinct product classes from a common, electrochemically generated hydrazine radical represents a rare example of electrochemically controlled radical divergence.

This platform is broadly applicable across 9 carbazates and delivers 35 examples, including functionalized and pharma-

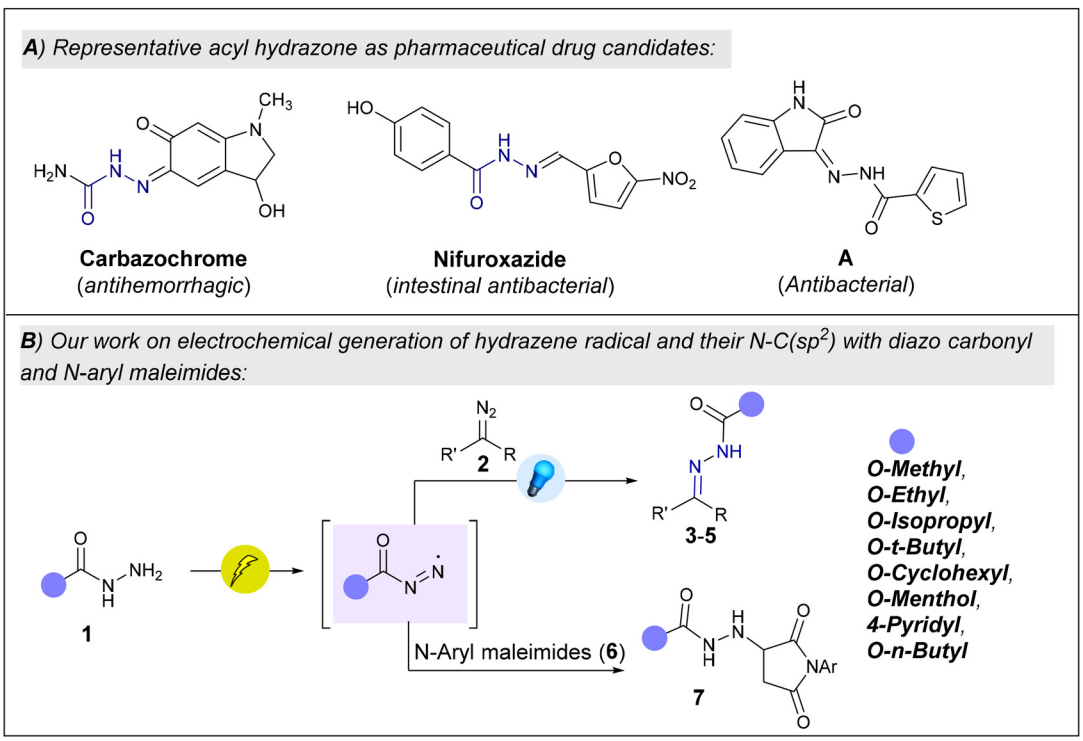

Scheme 1 (A) Representative acyl hydrazone-containing pharmaceuticals; (B) electrochemical generation of a diazene-centred radical and its C(sp^2)–N coupling with diazo carbonyls and *N*-aryl maleimides.

ceutically relevant scaffolds. Importantly, all transformations proceed without external reductants, transition metals, or Brønsted acids/bases, relying exclusively on electricity to orchestrate hydrazine radical generation and downstream bond formation. Collectively, this work provides a general, sustainable, and operationally straightforward strategy for constructing hydrazine-containing motifs and opens new avenues for exploring hydrazine reactivity in electrochemical synthesis.

To the best of our knowledge, the direct interception of an *in situ*–generated diazene radical with a diazo carbonyl species to construct *N*-acyl hydrazones, representing a formal coupling of a diazene radical with a radical anion to forge a C(sp^2)–N bond—has no precedent. This mechanistic combination thus defines a new bond-forming paradigm that expands both diazo chemistry and diazene-radical reactivity, motivating the study presented herein.[9]

Results and discussion

Our reaction design takes direct inspiration from the mechanistic framework established by Taniguchi and co-workers, who showed that alkyl carbazates undergo iron(III)-mediated single-electron oxidation to generate N-centered radical cations, which can evolve into diazene intermediates and ultimately fragment to alkoxycarbonyl radicals under aerobic conditions.[23] This study demonstrated that carbazates are intrinsically redox-responsive scaffolds, capable of accessing a sequence of nitrogen-centred intermediates under appropriate oxidative stimuli. Building on this logic, we envisioned that electrochemical oxidation a tunable, reagent-free analogue of Fe(III)/O_2 oxidation—could provide precise control over the *early* stages of this manifold. Specifically, by carefully modulating the oxidative window under constant-current electrolysis (DC or rAP), we sought to generate the initial hydrazine-centred N-radical for diazene radical formation while preventing its undesired progression toward acyl radical fragmentation.

Although oxidative electrochemical activation of carbazates has been reported in related anodic fragmentation studies—including the anodic pathways subtly exemplified by Gao and co-workers—such systems typically operate at unrestricted or higher oxidative potentials, thereby favouring diazene formation and onward N_2 extrusion.[34] In contrast, our design deliberately restricts the oxidative potential such that the diazene N-radical can be selectively formed and intercepted before further decomposition occurs. Critically, we reasoned that this N-centred intermediate could be strategically diverted into productive bond formation through two distinct radical-trapping pathways: (i) radical–carbene anion coupling with *in situ* generated carbene anions from aryl diazoacetates, and (ii) electrochemically promoted Michael-type conjugate addition to *N*-aryl maleimides. Thus, by integrating Taniguchi's mechanistic blueprint with the unique tunability of electrochemical oxidation, we established a proof-of-concept platform in which a diazene-centred radical can be both selectively generated and productively captured, enabling the divergent transformations disclosed herein.

We initiated our optimisation studies with an electro-photochemical strategy, anticipating that anodic oxidation of **2a** would generate the corresponding diazene radical *in situ*, which could subsequently engage with the electro-photochemically generated radical anion derived from the diazo compound. Encouragingly, under constant current electrolysis (5 mA) employing a carbon cathode and platinum anode in DMSO (0.1 M n-Bu_4NPF_6) with blue LED irradiation (456 nm) at 50–55 °C, the desired *N*-acyl hydrazone **3a** was obtained in 81% yield within 6 h (Scheme 2c). At room temperature, however, the reaction proceeded more slowly and delivered **3a** in only 45% yield over the same period (Scheme 2c, entry 5).

A systematic evaluation of reaction parameters underscored the importance of each component. Alternative light sources (green LED, white LED, UV) did not improve the outcome (Scheme 2c, entries 2–4). Conducting the reaction under air diminished the yield to 45% (entry 6), and replacing the carbon/platinum electrodes with nickel foam resulted in negligible conversion (entry 7). Substitution of the supporting electrolyte with *n*-Bu_4NCl or Me_4NBF_4 led to reduced efficiencies (64% and 73%, respectively; entries 8 and 9), while increasing the current to 10 mA caused partial product decomposition (entry 10). Notably, omission of blue light halted the reaction, highlighting the cooperative requirement for both electrochemical and photochemical activation (entry 11).

Under the optimised conditions—phenyl diazoacetate **1a** and methyl carbazate **2b** in DMSO (0.1 M *n*-Bu_4NPF_6), constant current electrolysis at 5 mA using carbon (–) and platinum (+) electrodes, blue LED irradiation (456 nm) at 50–55 °C under argon for 5–8 h—the transformation proceeds reliably to furnish *N*-acyl hydrazones *via* radical-mediated C(sp^2)–N bond formation. This dual-activation platform thus provides a practical and sustainable entry to hydrazone scaffolds.

With the optimized electrochemical conditions for diazene-radical generation in hand, we next evaluated the generality of the resulting formal C(sp^2)–N bond-forming process. As summarized in Scheme 3, controlled anodic oxidation of carbazates **1** in the presence of aryl diazoesters **2** enabled efficient radical–carbene anion coupling, affording a broad range of *N*-acyl hydrazones **3** under catalyst-, oxidant-, and base-free conditions. The electrochemically generated diazene radical was consistently intercepted across structurally varied substrates, delivering the desired products in moderate to excellent yields and highlighting the robustness and synthetic versatility of this electrochemical platform.

Initially, the scope of the reaction was examined using *tert*-butyl carbazate **2a** with various aryl diazoesters **1** bearing both electron-withdrawing and electron-donating substituents (Scheme 3). The reaction tolerated thiophene, halogen (Br/Cl) and cyano groups, affording the corresponding products (**3c**–**3e**) in 71–80% yields. Extension to heteroaromatic diazoesters, such as 2-thienyl-substituted analogue **1b**, also furnished the desired *N*-acyl hydrazone (**3b**) in 79% yield, highlighting the broad compatibility of this protocol (Scheme 3).

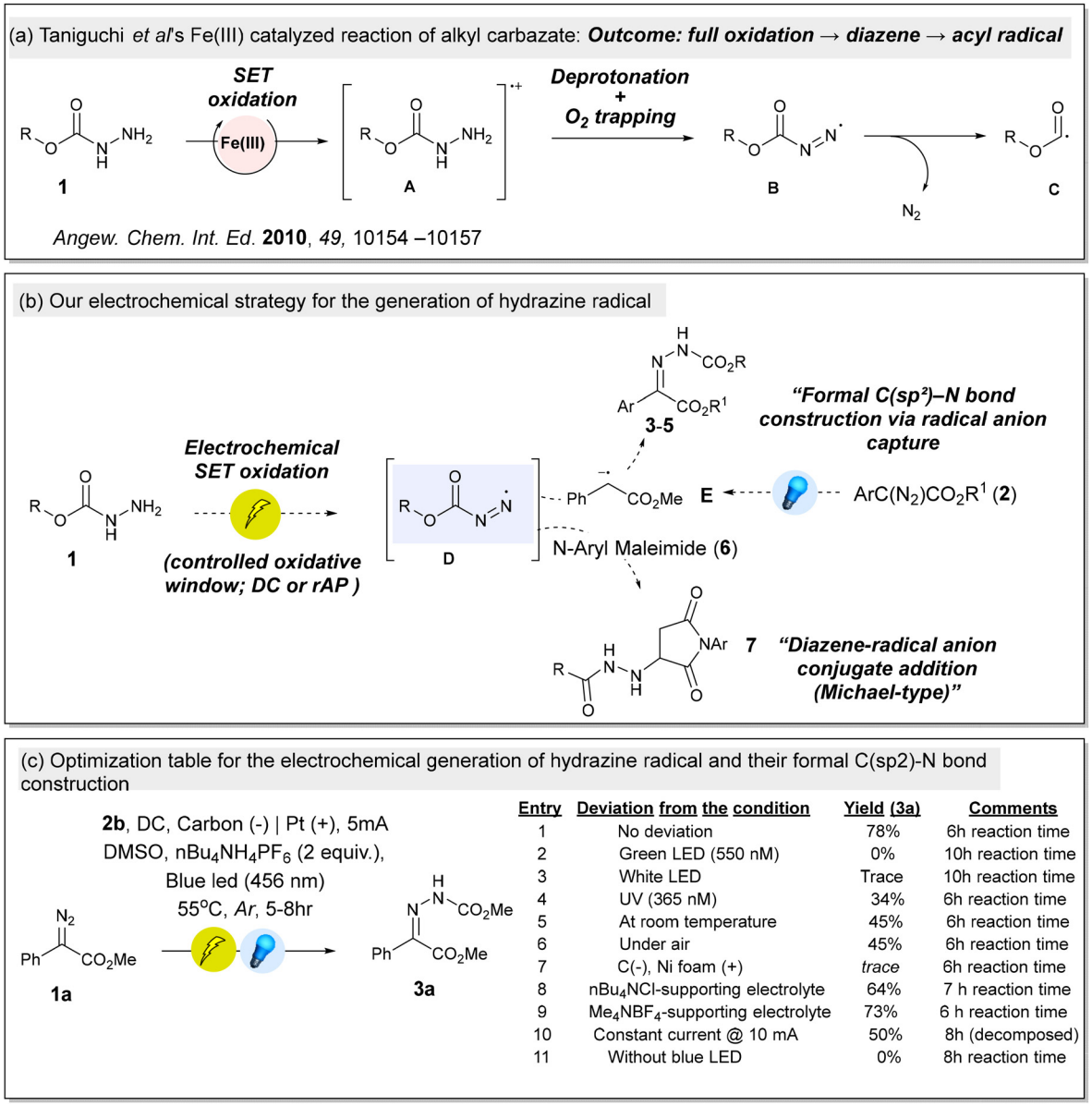

Entry	Deviation from the condition	Yield (3a)	Comments
1	No deviation	78%	6h reaction time
2	Green LED (550 nM)	0%	10h reaction time
3	White LED	Trace	10h reaction time
4	UV (365 nM)	34%	6h reaction time
5	At room temperature	45%	6h reaction time
6	Under air	45%	6h reaction time
7	C(-), Ni foam (+)	*trace*	6h reaction time
8	nBu_4NCl-supporting electrolyte	64%	7 h reaction time
9	Me_4NBF_4-supporting electrolyte	73%	6 h reaction time
10	Constant current @ 10 mA	50%	8h (decomposed)
11	Without blue LED	0%	8h reaction time

Scheme 2 (a) Fe(III)-mediated oxidation of alkyl carbazates (Taniguchi *et al.*); (b) electrochemical generation and interception of a diazene-centred N-radical (this work); (c) optimisation of electrochemical conditions for C(sp^2)–N bond formation to acyl hydrazones.

Encouraged by these results, a series of alkyl carbazates was next examined (Scheme 3). Methyl carbazate proved highly effective, giving hydrazones (**3a** and **3f–3h**) in 79–85% yields, irrespective of electronic effects on the aryl ring. Similarly, ethyl carbazate derivatives provided excellent yields (**3i–3l**, 70–80%), confirming that both steric and electronic variations on the carbazate were well tolerated (Scheme 3).

Further exploration with *isopropyl* and *menthol* carbazates demonstrated that sterically hindered and chiral carbazates also participated efficiently, affording the corresponding products (**3m–3o**) in 69–76% yields (Scheme 3). Notably, the reaction was successfully extended to *isoniazid*-derived carbazates, affording a range of pharmaceutically relevant *N*-acyl hydrazones (**3p–3t**) in 70–86% yields (Scheme 3). These results underscore the potential of this electro-photochemical approach for late-stage functionalization of drug-like molecules. The molecular structure of representative hydrazone **3q** unambiguously confirmed by single-crystal X-ray diffraction analysis.

Additionally, cyclic and benzylic carbazates further broadened the substrate scope (Scheme 3). Cyclohexyl carbazate provided the corresponding *N*-carbamoyl hydrazone (**3u**) in 79% yield (Scheme 3). Notably, when benzyl carbazate was employed, the reaction furnished the *N*-benzyl hydrazone (**3v**) in 59% yield, indicating retention of the *N*-benzyl moiety rather than formation of an *N*-carbobenzoxy derivative. Similarly, *n*-butyl carbazate **2i** when reacted with phenyl diazo acetate **1a** under the optimized condition afforded the desired

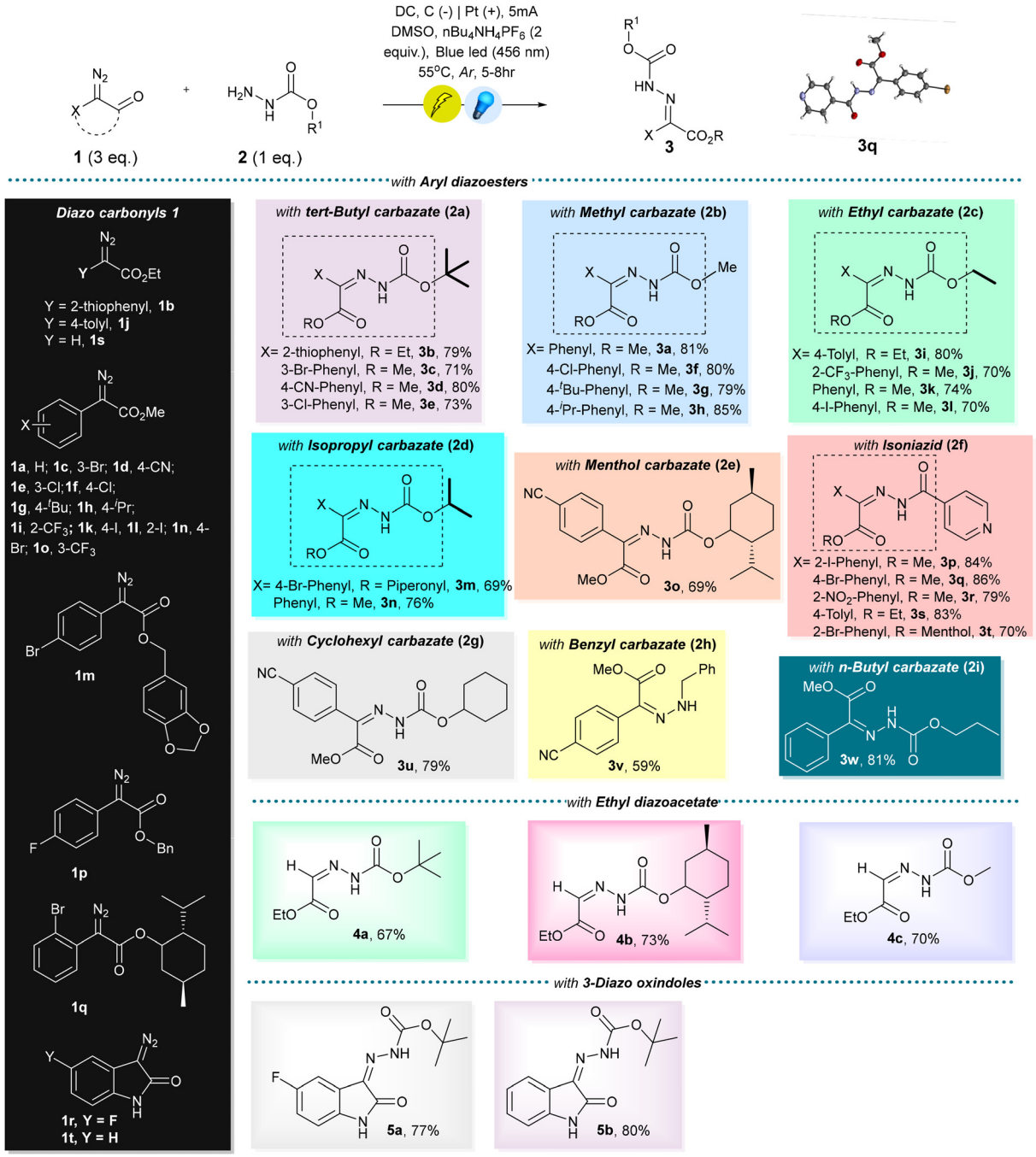

Scheme 3 Substrate and reagent scope of the electro-photochemical *N*-acyl hydrazone synthesis. Reactions were conducted under argon for 5–8 h. Yields correspond to isolated products after chromatographic purification.

product **3w** in 81% yield (Scheme 3). Next, replacing aryl diazoesters with ethyl diazoacetate **1s** afforded the corresponding *N*-carbamoyl hydrazones (**4a–4c**) in 67–73% yields, thereby confirming the generality of the methodology beyond aromatic systems (Scheme 3).

Finally, it was gratifying to see that under our electro-photochemical strategy 5-fluoro-3-diazo oxindole **1r** and diazo oxindole **1t**, when reacted with **2a** afforded the desired oxindole-3-hydrazone **5a** and **5b** in 77 and 80% yield.

To verify the practical utility and scalability of the developed protocol, a gram-scale reaction was performed under the standard optimized conditions. To a stirred solution of **1a** (22.69 mmol, 3.0 equiv.) in 30 mL of DMSO 30 mL, **2a** (7.57 mmol, 1.0 equiv.) was added. The reaction afforded the desired product **3a** as a yellow viscous liquid (1.37 g, 65% yield).

Overall, this electro-photochemical protocol exhibits wide functional group tolerance, broad substrate applicability, and

operational simplicity, providing an efficient and sustainable route to structurally diverse *N*-acyl hydrazones under mild conditions.

Having established that carbazates can be selectively oxidized to generate a persistent diazene-centred radical, we next examined whether this platform could be extended to the direct functionalization of *N*-aryl maleimides. Guided by our reaction-design hypothesis (Scheme 2b), we anticipated that anodic oxidation of the carbazate would furnish the diazene radical, which could undergo Michael-type conjugate addition across the electron-deficient C═C bond of an *N*-aryl maleimide, ultimately affording the corresponding succinimide-linked hydrazine.

Initial optimization studies for the maleimide conjugation were conducted using constant current (DC) electrolysis with *tert*-butyl carbazate **2a** (Table 1, entry 8). While phenyl maleimide **4a** provided moderate yields (35%), the reaction stalled or failed completely for substituted derivatives. Visual inspection of the carbon cathode revealed the fouling of electrode, suggesting that electrode passivation was the primary failure mode. To circumvent this surface blocking, we transitioned from static DC to a Rapid Alternating Polarity (rAP) waveform. We hypothesized that the periodic polarity reversal would mitigate fouling.

Next, the reaction parameters were systematically evaluated to identify conditions that efficiently promote diazene-radical interception while minimizing electrode passivation and decomposition (Table 1). Under the optimized conditions (rAP electrolysis, graphite cathode|graphite anode, DMSO, *n*-Bu_4NPF_6), the desired succinimide-linked hydrazine was obtained in 81% yield within 6 h (Table 1, entry 1), establishing this setup as a robust baseline.

Electrode material screening revealed that carbon-based cathodes are crucial for productive reactivity. Reversing electrode polarity (C(+)|Pt(−)) or employing platinum as both electrodes led to only marginal erosion of yield (Table 1, entries 2–4), indicating that the transformation is relatively tolerant to anodic materials but more sensitive to cathodic surface properties. In contrast, the use of stainless steel as the cathode completely shut down the reaction (Table 1, entry 5), likely due to rapid electrode fouling or competitive surface-mediated side reactions that suppress effective radical generation.

Atmospheric control proved essential: conducting the reaction under air resulted in a significant drop in yield to 30% (Table 1, entry 6), consistent with competitive quenching of radical intermediates by oxygen. Solvent effects were also pronounced; replacement of DMSO with dichloromethane led only to trace product formation (Table 1, entry 7), underscoring the importance of a polar, aprotic medium capable of stabilizing charged and radical intermediates under rAP conditions.

Finally, variation of the supporting electrolyte showed that n-Bu_4NPF_6 outperforms Me_4NBF_4 (Table 1, entry 9), likely due to improved ionic conductivity and interfacial charge transfer in DMSO.

Collectively, these optimization studies demonstrate that efficient formation of hydrazine-tethered succinimides relies on a delicate balance of electrode material, waveform control, solvent polarity, and inert atmosphere. The superiority of rAP electrolysis in particular underscores its role in mitigating electrode fouling and enabling sustained radical chemistry, a feature that is central to the success and generality of this divergent electrochemical platform.

In addition to the aforementioned direct radical-addition pathway, we also considered a complementary mechanistic route based on the intrinsic redox behaviour of the reaction partners. Under the electrochemical conditions, *N*-aryl maleimides are capable of accepting an electron to generate a maleimide radical anion, while the oxidized carbazate exists in equilibrium with its conjugate diazene carboxylate, the immediate precursor of the diazene radical. Product formation can therefore also arise from coupling between the maleimide radical anion and the diazene carboxylate, followed by protonation, providing an alternative and mechanistically consistent route to the same hydrazine-tethered succinimide products.

Together, these two complementary pathways—direct addition of the diazene radical and cross-coupling between the maleimide radical anion and diazene carboxylate—highlight the flexibility and inherent divergence of the electrochemical platform, enabling efficient construction of succinimide-linked hydrazine architectures from simple precursors.

Following the optimized rAP conditions shown in Table 1, rAP electrolysis (GF (−)|GF (+), 20 mA), DMSO, *n*Bu_4NPF_6 (0.1 M), Ar various alkyl carbazates **2** reacted efficiently with *N*-arylmaleimide **4** to give adduct **7** within 5–6 h (Scheme 4). The reaction proceeds cleanly under catalyst-, oxidant-, and base-free conditions, underscoring the operational simplicity of the electrochemical approach.

The scope of this radical conjugate-addition manifold was next explored using a range of electron-poor, electron-neutral,

Table 1 Optimization of electrochemical conditions for the coupling of *tert*-butyl carbazate **2a** with *N*-phenyl maleimide **4a** to afford hydrazine-tethered succinimides **7a** under rAP and DC electrolysis

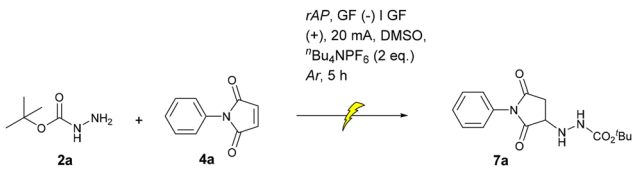

Entry	Deviation from the condition	Yield[a]	Comments
1	No deviation	81%	6 h reaction time
2	C (+) I Pt (−)	78%	6 h reaction time
3	Pt (+) I Pt (−)	74%	6 h reaction time
4	Pt (+) I RVC (−)	72%	6 h reaction time
5	Pt (+) I stainless steel (−)	0%	After 10 h
6	Under air	30%	6 h reaction time
7	DCM as solvent	Trace	6 h reaction time
8	Constant current (CCD)	35%	6 h (decomposed)
9	Me_4NBF_4 supporting electrolyte	68%	6 h reaction time

[a] Isolated yield.

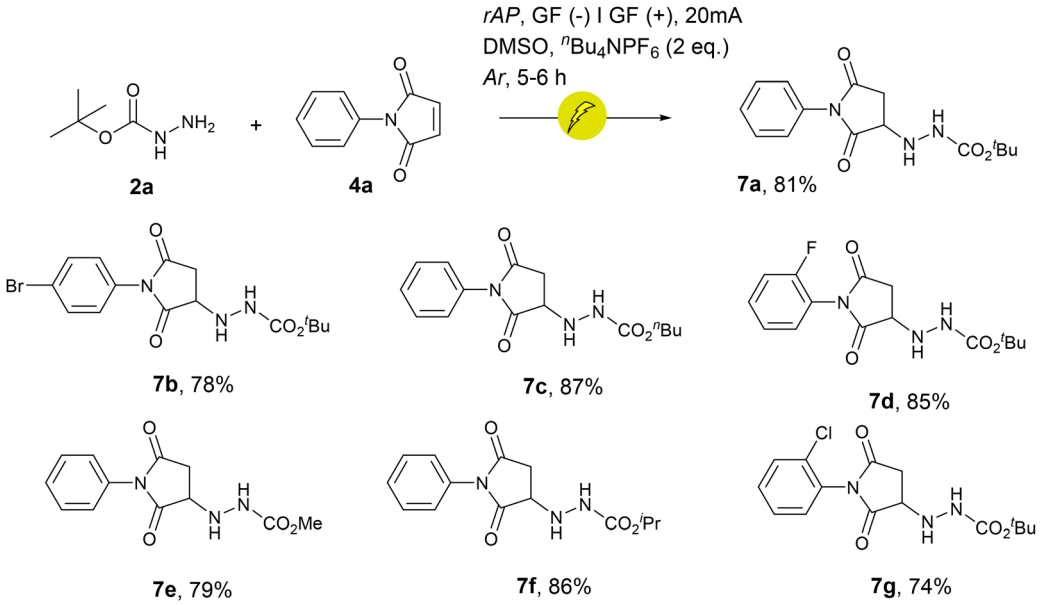

Scheme 4 Electrochemical generation of a hydrazine-centered N-radical enables direct Michael-type addition to *N*-aryl maleimides.

and electron-rich *N*-aryl maleimides, as well as different carbazate derivatives (**2a**, **2b**, **2d** and **2i**). As illustrated in Scheme 4, the method proved broadly general: *para*-bromo, *ortho*-fluoro, and *ortho*-chloro-substituted maleimides furnished the corresponding products (**7b**, **7d**, **7g**) smoothly, demonstrating tolerance to halogens commonly used as cross-coupling handles. Variation of the alkyl group on the carbazate revealed that *n*-butyl, methyl, and isopropyl carbazates also engaged efficiently, delivering the corresponding hydrazine adducts (**7c**, **7e**, **7f**) in good yields. Across these examples, the reaction consistently exhibited excellent chemoselectivity, with no detectable over-reduction or over-oxidation of the maleimide core.

Collectively, these results establish carbazate oxidation as a general electrochemical strategy for N-radical conjugate addition, enabling the facile construction of succinimide-linked hydrazines, structural motifs that are otherwise difficult to access through traditional nucleophilic or reductive methodologies. This divergent reactivity, accessible from the same hydrazine radical precursor used in our *N*-acyl hydrazone synthesis, further highlights the versatility of the electrochemically generated hydrazine radical and expands the synthetic potential of carbazates as redox-responsive nitrogen-transfer reagents.

To gain deeper insight into the mechanism of our electrochemical diazene-radical chemistry—including both the radical–radical anion coupling that produces *N*-acyl hydrazones (**3**–**5**) and the N-radical conjugate addition leading to succinimide-linked hydrazines (**7**), we carried out a series of diagnostic control experiments (Scheme 5). Our overarching goal was to determine whether the diazene-centred radical proposed in our reaction design is indeed generated under the optimized electrochemical conditions and whether this radical intermediate plays a decisive role in enabling both divergent product manifolds.

We first sought direct evidence for radical formation using a classical trapping experiment. When carbazate **1a** was exposed to the electrochemical conditions in the presence of BHT, the corresponding BHT-adduct **E** was detected by HRMS (Scheme 5a). This adduct is consistent with interception of an N-centred hydrazine-derived radical, providing direct, experimentally observed support for our mechanistic hypothesis. The formation of **E** gave us early confidence that anodic oxidation of **1a** indeed proceeds through a radical pathway.

Next, we examined the behaviour of carbazate **1a** in the absence of any coupling partner. Under the optimized electrochemical conditions—without diazoester **2a** or maleimide **4a**—1a underwent dimerization to afford isolable product **8** (Scheme 5b). Its structure was confirmed by NMR and HRMS. Such dimer formation is fully consistent with a persistent, freely diffusing N-centred radical generated from **1a** when no external trapping agent is available, reinforcing the notion that radical intermediates play a central role in this chemistry.

We then evaluated the effect of radical traps on both reaction pathways. For the hydrazone-forming reaction, the addition of TEMPO (2 equiv.) or DMPO (2 equiv.) suppressed formation of **3a** to 15%, along with the TEMPO–diazo-derived adduct **F** and 19%, along with the DMPO-carbazate adduct **F**[1] was detected (Scheme 5c_1 and c_2). These observations strongly support the involvement of a radical anion, which is well known to be intercepted by TEMPO and the generation of a diazene radical intercepted by DMPO. Similarly, for the maleimide pathway, addition of TEMPO reduced the yield of **7a** to 18% and led to detection of TEMPO-adduct **G** (Scheme 5d). The parallel behaviour of both systems provides compelling evidence that each manifold proceeds through radical intermediates.

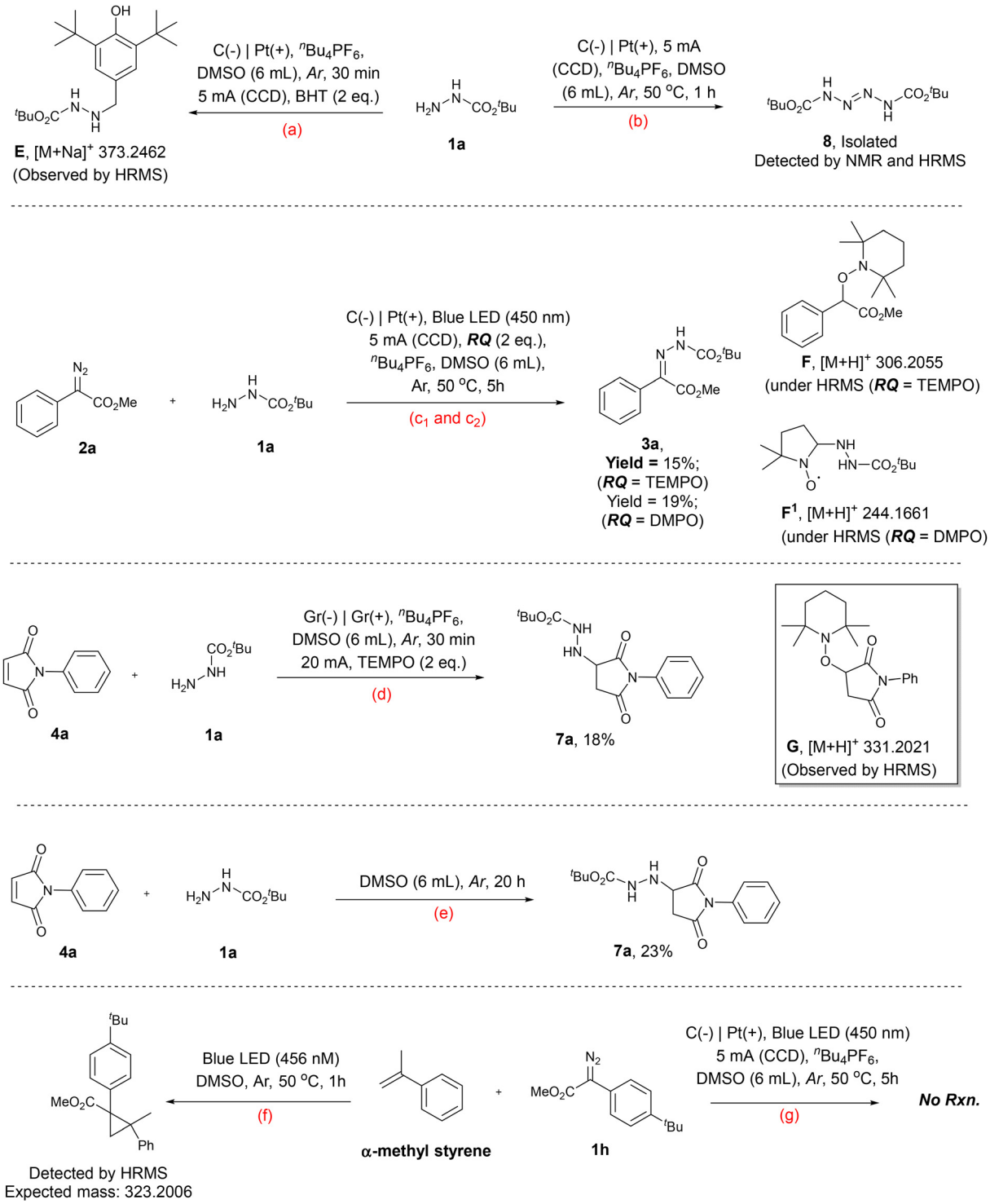

Scheme 5 Probing the electrochemical oxidative window of carbazates: (a) BHT trapping of the N-centred radical from **1a**; (b) dimerisation of **1a** to **8** without coupling partners; (c) TEMPO/DMPO suppression of hydrazone formation and detection of adducts **F** and **F**^{1}; (d) TEMPO inhibition of the maleimide pathway (adduct **G**); (e) low conversion without electrolysis; (f) trapping evidence for carbene radical anion formation.

To probe whether thermal activation alone could account for the observed products, we carried out a control reaction in the absence of electricity. When **1a** and **4a** were stirred in DMSO at r.t. under argon, the hydrazine–maleimide coupling product **7a** did form, but only in 23% yield after 20 h (Scheme 5e). In stark contrast, the electrochemical variant delivers the same product in only 5–6 h. These results highlight the enabling role of electro-

chemical oxidation in accessing the hydrazine radical efficiently and selectively.

To further elucidate the nature of the reactive species generated under our electro-photochemical conditions, we conducted a series of control experiments using α-methylstyrene as a diagnostic chemical trap (Scheme 5f and g). It is well-established that aryl diazoacetates liberate nitrogen to generate carbenes under photochemical stimulation, which typically engage in [2 + 1] cycloaddition with alkenes to yield cyclopropanes. This was observed in the reaction of **1h** with α-methyl styrene and blue LED only (Scheme 5f). Whereas the absence of cyclopropanation (no reaction at all!) under our standard electro-photochemical conditions (Scheme 5g) provides compelling evidence that the reaction does not proceed *via* a free carbene. Instead, we propose that the combination of light and electricity facilitates a Single Electron Transfer (SET) process. In this pathway, the aryl diazoacetate is reduced to a radical anion.

A critical question was whether the reaction required the paired electrochemical activation of both partners, or whether the anodic process alone was sufficient. To elucidate this and the mechanistic roles of the key reagents and distinguish between oxidative and reductive initiation pathways, we conducted control experiments in a divided H-cell separated by a Nafion membrane (Scheme 6a). Special care was taken to balance the half-reactions in the counter-chambers to ensure consistent current flow (5 mA) and prevent kinetic bottlenecks. In the first experiment, the anodic chamber was charged with the standard reaction mixture (**1a** and **2a**), while the cathodic counter-chamber contained the electrolyte solution with added methanol. The methanol served as a proton source to facilitate the Hydrogen Evolution Reaction (HER) at the cathode, ensuring efficient electron flow. Under these conditions, the desired product was isolated in 3% yield. Conversely, when the reaction mixture was placed in the catho-

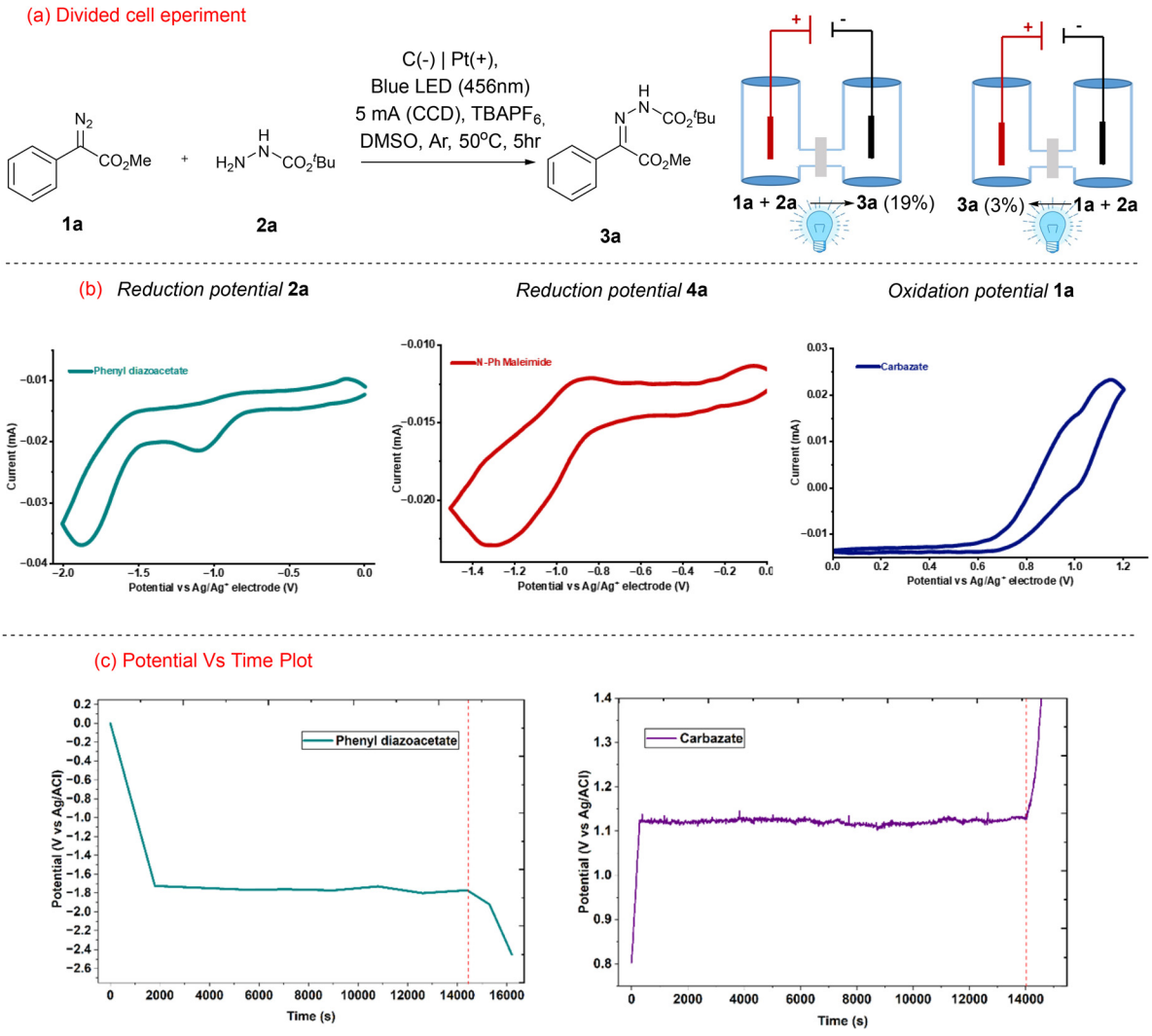

Scheme 6 (a) Divided-cell electrolysis suppresses product formation, indicating the requirement for paired anodic and cathodic activation (H-cell, Nafion membrane). (b) Chronopotentiometry defining operational potentials of **1a** and **2a**. (c) CV analysis showing oxidation of **1a** and reduction of diazoester **2a** and maleimide **4a**.

dic chamber, a sacrificial copper wire was employed as the anode in the counter-chamber to balance the circuit *via* facile copper oxidation. Despite the identical electrical current and light irradiation, this setup resulted in a significantly diminished yield of 19%.

This finding demonstrates that anodic oxidation of the carbazate alone is not sufficient to drive the transformation. Instead, successful product formation requires the simultaneous cathodic reduction of the diazo partner—supporting the mechanistic model in which the diazo compound accepts an electron to generate a diazo radical anion, which then undergoes N_2 loss to produce the carbene anion radical that couples with the diazene radical. The divided-cell experiment therefore provides strong functional evidence that both electrodes contribute essential reactive species, confirming that the hydrazone formation proceeds through a paired electrochemical radical manifold.

Next, we turned to cyclic voltammetry to map the relevant redox processes (Scheme 6b). Carbazate **1a** displayed a clean, irreversible oxidation between +1.0 and +1.1 V *vs.* Ag/Ag^+, consistent with facile generation of the hydrazine-centred radical. In contrast, both diazoester **2a** and maleimide **4a** exhibited reductive features (−1.75 V and −1.25 V, respectively), indicating that both substrates can be activated at the cathode. Reduction of **2a** is consistent with formation of a diazo radical anion, leading rapidly to a carbene anion radical, whereas reduction of **4a** affords a persistent maleimide radical anion capable of reacting with the diazene carboxylate or diazene radical.

Next the progress of the reaction between **1a** and **2a** was investigated by monitoring the cathodic and anodic potentials over time and then the progress was plotted against time (Scheme 6c). We observed that during the reaction, the cathodic potential was maintained around −1.7 V *vs.* Ag/Ag^+ reference electrode, and the anodic potential was maintained around 1.1 V *vs.* Ag/Ag^+ reference electrode. From the CV experiment we also observed that the peak reduction potential for **2a** was −1.75 V and peak reduction potential for **1a** was in a range of +1.0 V to +1.1 V. These results stipulated that during the reaction, **2a** was reduced at cathode and **1a** was oxidised at anode which consumed towards product formation. When both the substrates were consumed fully then the both the cathodic and anodic potentials were started increasing indicating the completion of the reaction which is consistent with the overall reaction duration as well.

Together, these mechanistic experiments, including radical traps, substrate-free controls, thermal comparisons, cyclic voltammetry, and, critically, the divided-cell study, paint a unified picture in which paired electrochemical activation generates two complementary reactive partners: (1) an anodically formed diazene-centred N-radical, and (2) a cathodically generated carbene anion radical or maleimide radical anion.

The convergence of these species enables two distinct yet interconnected reaction pathways, validating the core design principle of our electrochemical platform and showcasing the versatility of controlled electrochemical radical generation in directing divergent C–N bond-forming chemistry.

Guided by the results of our control experiments, we propose the mechanistic model illustrated in Scheme 7 to rationalize the formation and divergent reactivity of the electrochemically generated hydrazine-derived radicals. The sequence begins with successive anodic oxidations of carbazate **1**, which furnish the N-centered radical cation **A**. Deprotonation of **A** gives the neutral hydrazine radical $\mathbf{A^1}$, which undergoes a second oxidation/deprotonation event to provide both the diazene carboxylate $\mathbf{A^2}$ and its corresponding diazene-centered radical **B**. These two species $\mathbf{A^2}$ and **B**, constitute the key reactive intermediates that diverge toward the two product classes observed in this work (Scheme 7).

In the *N*-acyl hydrazone pathway (**3–5**), the aryl diazoesters undergo cathodic reduction to generate the diazo-derived radical anion **H**. This species readily extrudes N_2 to form a radical anion that couples with the diazene-centered radical **B**, leading to the formal $C(sp^2)$–N bond formation that characterizes the *N*-acyl hydrazone products (Scheme 7).

In the maleimide functionalization pathway (product class **7**), the *N*-aryl maleimides **4** undergo electrochemical reduction at the cathode to generate the corresponding radical anion **K**. This electrophilic π-radical species engages with the nucleophilic diazene carboxylate $\mathbf{A^2}$, producing intermediate **L**, which is then protonated to furnish the succinimide-linked hydrazine product **7**. The observation that this reaction proceeds rapidly only under electrochemical conditions underscores the essential role of the cathodic reduction step in activating the maleimide toward radical conjugate addition (Scheme 7).

Control experiments revealed a distinct divergence in the activation requirements of the two reaction manifolds (Scheme 6). The hydrazone-forming pathway was found to proceed efficiently only under simultaneous electrolysis and blue LED irradiation, whereas omission of light resulted in negligible conversion. In contrast, the conjugate addition to *N*-aryl maleimides proceeded smoothly under electrochemical conditions in the absence of any photochemical input.

This difference can be rationalised by the role of the diazo partner. In the hydrazone pathway, photochemical activation of the aryl diazoacetate is required to promote N_2 extrusion and generate a reactive carbene (or carbene radical anion) capable of coupling with the electrochemically generated diazene-centred radical. Without light, the diazo compound remains insufficiently activated for productive radical engagement. By contrast, the maleimide pathway involves direct Michael-type addition of the diazene radical to an electron-deficient alkene and therefore does not require photochemical activation.

Accordingly, light is specifically required for diazo activation in the coupling manifold, whereas the conjugate addition proceeds *via* a purely electrochemically driven radical process.

Taken together, these mechanistic insights highlight how a single electrochemically generated nitrogen-centred manifold —originating from the oxidation of carbazates—can give rise to two distinct yet complementary reactivity pathways, depending on the nature of the substrate present at the cathode. This

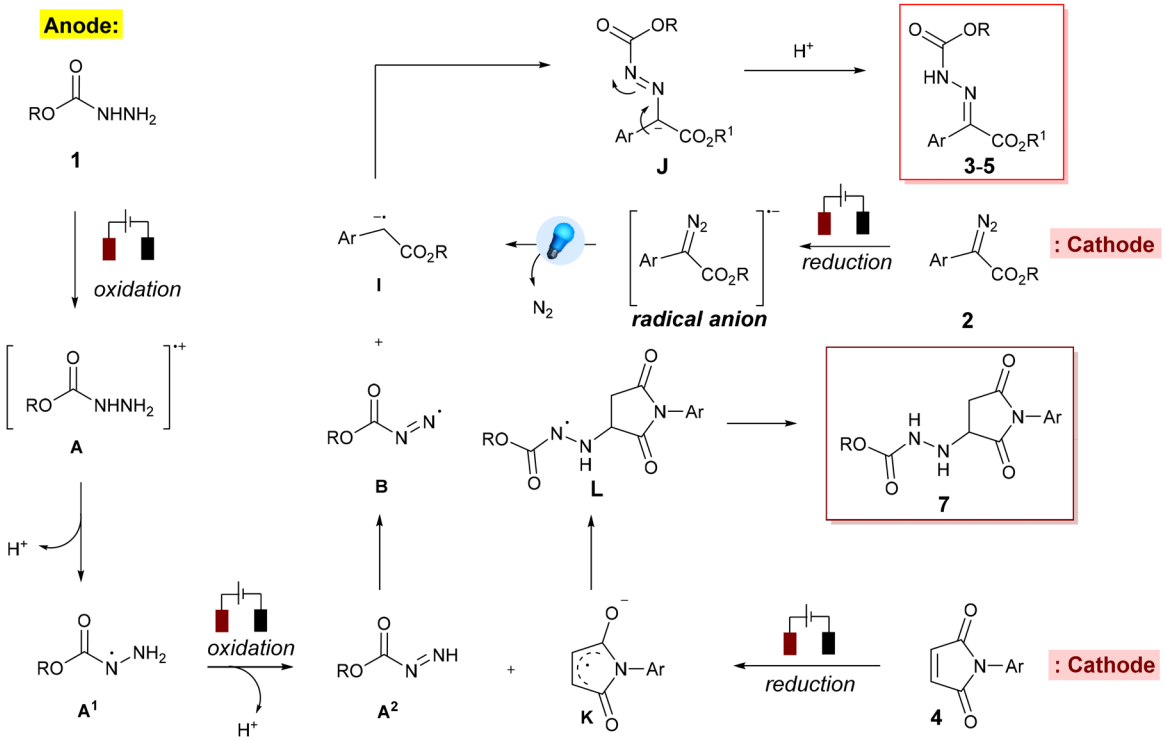

Scheme 7 Unified mechanistic model highlighting diazene-derived N-radicals and their divergent reactivity.

interplay between anodic radical generation and cathodic substrate activation lies at the heart of the divergent hydrazine radical chemistry uncovered in this study.

Conclusion

In conclusion, this work demonstrates that electricity alone can be used to unlock the reactivity of common carbazates and turn them into a diazene-centred nitrogen radical, a species that is normally difficult to access safely or selectively. By relying on anodic oxidation rather than metals, oxidants, or hazardous hydrazine reagents, we provide a clean and sustainable way to generate this highly reactive intermediate using nothing more than benign starting materials and controlled electrochemical input.

What makes this platform particularly exciting is how flexibly this diazene radical can be guided toward different outcomes. By pairing the radical with appropriately activated partners, we were able to create two completely distinct classes of products from the very same intermediate. Under electro-photochemical conditions, aryl diazo acetates are reduced to a radical anion, which couples smoothly with the diazene radical to form *N*-acyl hydrazones. This transformation uncovers a reactivity mode for diazo compounds that goes well beyond their traditional roles in carbene chemistry and opens a new route for forming C(sp^2)–N bonds under exceptionally mild conditions.

It is noteworthy, traditional syntheses of *N*-acyl hydrazones mainly rely on two-electron chemistry, most often the acid- or base-mediated condensation of acyl hydrazides with carbonyl compounds. While effective, these methods are equilibrium-driven, can require heating or additives, and often show limited tolerance toward sensitive or redox-active functional groups. In contrast, the electro-photochemical strategy reported here constructs *N*-acyl hydrazones through a fundamentally different single-electron pathway. Anodic oxidation of carbazates generates a persistent diazene-centred N-radical, which couples directly with a cathodically formed diazo-derived radical anion after N_2 extrusion. This avoids classical condensation chemistry altogether and enables direct C(sp^2)–N bond formation under mild, catalyst-free, and acid/base-free conditions. Beyond improved sustainability, the key advantage of this approach lies in its orthogonal reactivity: substrates such as diazo esters, heterocycles, and drug-derived carbazates that are challenging for conventional methods are readily accommodated. As such, the electro-photochemical platform is not merely a greener alternative, but a new reactivity paradigm for accessing *N*-acyl hydrazones.

In a complementary pathway, when *N*-aryl maleimides are used instead, their cathodic reduction generates reactive radical anions that undergo a Michael-type addition with the diazene radical. This leads to hydrazine-tethered succinimides, structures of importance in medicinal chemistry and molecular design. The fact that a single nitrogen radical can be steered toward either radical anion coupling or radical conjugate addition simply by changing the trapping partner highlights the precision and versatility that electrochemistry can bring to synthetic design.

Together, these results demonstrate how combining electrochemical oxidation, electrochemical reduction, and photochemical activation can uncover reaction pathways that are otherwise difficult to achieve. By transforming stable carbazates into useful nitrogen radicals and showing how they can be intercepted in two different ways, we hope to broaden the synthetic community's view of what nitrogen-centred radicals can accomplish under sustainable, catalyst-free conditions.

We anticipate that this divergent radical strategy will serve as a foundation for future methods that use electricity to gently "turn on" new types of nitrogen reactivity, enabling the construction of diverse hydrazine-containing architectures and beyond.

Conflicts of interest

There are no conflicts to declare.

Data availability

The supporting data has been provided as part of the supplementary information (SI). Supplementary information: Table S1, Scheme S1 and Fig. S1–S5, NMR spectra and further experimental details. See DOI: https://doi.org/10.1039/d6qo00078a.

CCDC 2346164 contains the supplementary crystallographic data for this paper.[35]

Acknowledgements

This work was supported by ANRF CRG research grant (CRG/2023/001272) from DST-SERB India for fund support.

References

1 H. H. Sisler, G. M. Omietanski and B. Rudner, The chemistry of quaternized hydrazine compounds, *Chem. Rev.*, 1957, **57**, 1021–1047.
2 U. Ragnarsson, Synthetic methodology for alkyl substituted hydrazines, *Chem. Soc. Rev.*, 2001, **30**, 205–213.
3 S. Rollas and S. Küçükgüzel, Biological activities of hydrazone derivatives, *Molecules*, 2007, **12**, 1910–1939.
4 L. Wei, S. Ding, M. Liu, Z. Yu and Y. Xiao, Synthesis of trifluoromethylated pyrazolidines, pyrazolines and pyrazoles via divergent reaction of β-CF_3–1,3-enynes with hydrazines, *Org. Lett.*, 2021, **23**, 7718–7723.
5 Y. Zhang, K. Li, W. Gao, X. Liu, H. Yuan, L. Tang and Z. Fan, Tandem synthesis of 1,2,3-thiadiazoles with 3,4-dichloroisothiazoles and hydrazines under external oxidant- and sulfur-free conditions, *Org. Lett.*, 2022, **24**, 6599–6603.
6 J. M. Sayer, B. Pinsky, A. Schönbrunn and W. Washtien, Mechanism of carbinolamine formation, *J. Am. Chem. Soc.*, 1974, **96**, 7998–8009.
7 M. Xiao, J. Ye, W. Lian, M. Zhang, B. Li, A. Liu and A. Hu, Microwave-assisted synthesis, characterization and bioassay of acylhydrazone derivatives as influenza neuraminidase inhibitors, *Med. Chem. Res.*, 2017, **26**, 3216–3227.
8 M. M. Andrade and M. T. Barros, Fast synthesis of N-acylhydrazones employing a microwave assisted neat protocol, *J. Comb. Chem.*, 2010, **12**, 245–247.
9 M. Pérez-Venegas and E. Juaristi, Mechanochemical and mechanoenzymatic synthesis of pharmacologically active compounds: a green perspective, *ACS Sustainable Chem. Eng.*, 2020, **8**, 8881–8893.
10 C. G. Ávila-Ortiz and E. Juaristi, Novel methodologies for chemical activation in organic synthesis under solvent-free reaction conditions, *Molecules*, 2020, **25**, 3579.
11 E. Yasui, M. Wada and N. Takamura, Efficient solid-phase synthesis of N-acylhydrazones, *Chem. Pharm. Bull.*, 2007, **55**, 1652–1654.
12 C. Liu, *et al.*, Expedient synthesis of E-hydrazone esters and 1H-indazole scaffolds through heterogeneous single-atom platinum catalysis, *Sci. Adv.*, 2019, **5**, eaay1537.
13 J. Huo, Y. Xue and J. Wang, Regioselective copper-catalyzed aminoborylation of styrenes with bis(pinacolato)diboron and diazo compounds, *Chem. Commun.*, 2018, **54**, 12266–12269.
14 S. Z. Zard, Recent progress in the generation and use of nitrogen-centred radicals, *Chem. Soc. Rev.*, 2008, **37**, 1603–1618.
15 T. Xiong and Q. Zhang, New amination strategies based on nitrogen-centered radical chemistry, *Chem. Soc. Rev.*, 2016, **45**, 3069–3087.
16 J.-R. Chen, X.-Q. Hu, L.-Q. Lu and W.-J. Xiao, Visible light photoredox-controlled reactions of N-radicals and radical ions, *Chem. Soc. Rev.*, 2016, **45**, 2044–2056.
17 M. D. Kärkäs, Photochemical generation of nitrogen-centered amidyl, hydrazonyl and imidyl radicals: methodology developments and catalytic applications in synthesis, *ACS Catal.*, 2017, **7**, 4999–5022.
18 J. Davies, S. P. Morcillo, J. J. Douglas and D. Leonori, Hydroxylamine Derivatives as Nitrogen-Radical Precursors in Visible-Light Photochemistry, *Chem. – Eur. J.*, 2018, **24**, 12154–12163.
19 X.-Y. Yu, Q.-Q. Zhao, J. Chen, W.-J. Xiao and J.-R. Chen, When light meets nitrogen-centered radicals: from reagents to catalysts, *Acc. Chem. Res.*, 2020, **53**, 1066–1083.
20 G. Kumar, S. Pradhan and I. Chatterjee, Recent advances in N-radical-mediated C–H functionalization of amides, *Chem. – Asian J.*, 2020, **15**, 651–672.
21 P. Wang, Q. Zhao, W. Xiao and J. Chen, Recent advances in visible-light photoredox-catalyzed nitrogen radical cyclization, *Green Synth. Catal.*, 2020, **1**, 42–51.
22 C. Pratley, S. Fenner and J. A. Murphy, Nitrogen-centered radicals in functionalization of sp^2 systems: generation, reactivity and applications in synthesis, *Chem. Rev.*, 2022, **122**, 8181–8260.
23 T. Taniguchi, Y. Sugiura, H. Zaimoku and H. Ishibashi, Iron-Catalyzed Oxidative Addition of Alkoxycarbonyl

Radicals to Alkenes with Carbazates and Air, *Angew. Chem., Int. Ed.*, 2010, **49**, 10154–10157.
24 D. Pollok and S. R. Waldvogel, Electro-organic synthesis – a 21st century technique, *Chem. Sci.*, 2020, **11**, 12386–12400.
25 H. R. Stephen and J. L. Röckl, The future of electro-organic synthesis in drug discovery and early development, *ACS Org. Inorg. Au*, 2024, **4**, 571–578.
26 C. Zhu, N. W. J. Ang, T. H. Meyer, Y. Qiu and L. Ackermann, Organic electrochemistry: molecular syntheses with potential, *ACS Cent. Sci.*, 2021, **7**, 415–431.
27 Z. Zhang and V. Gevorgyan, Visible light-induced reactions of diazo compounds and their precursors, *Chem. Rev.*, 2024, **124**, 7214–7261.
28 F. Doraghi, P. Baghershahi, M. Ghasemi, M. Mahdavi and A. Al-Harrasi, Rhodium-catalyzed transformations of diazo compounds via a carbene-based strategy: recent advances, *RSC Adv.*, 2024, **14**, 39337–39352.
29 J. Durka, J. Turkowska and D. Gryko, Lightening diazo compounds?, *ACS Sustainable Chem. Eng.*, 2021, **9**, 8895–8918.
30 F. Zhao, H. Ding, T. Sun, C. Shen, Z.-L. Wang, W. Wei and D. Yi, Visible-light-promoted multicomponent carbene transfer reactions, *Chin. Chem. Lett.*, 2026, **37**, 111834.
31 H. A. Khan, M. Szostak and C. Sivasankar, Diazo compounds: synthesis, carbene generation and reactivity, *Org. Biomol. Chem.*, 2026, **24**, 734–766.
32 S. Küçükgüzel, A. Mazi, F. Şahin, S. Öztürk and J. Stables, Synthesis and biological activities of diflunisal hydrazide-hydrazones, *Eur. J. Med. Chem.*, 2003, **38**, 1005–1013.
33 D. Ramimoghadam, D. J. Eyckens, R. A. Evans, G. Moad, S. Holmes and R. Simons, Towards sustainable materials: a review of acylhydrazone chemistry for reversible polymers, *Chem. – Eur. J.*, 2024, **30**, e202401728.
34 Y. Gao, Z. Wu, L. Yu, Y. Wang and Y. Pan, Alkyl carbazates for electrochemical deoxygenative functionalization of heteroarenes, *Angew. Chem., Int. Ed.*, 2020, **59**, 10859–10863.
35 CCDC 2346164: Experimental Crystal Structure Determination, 2026, DOI: **10.5517/ccdc.csd.cc2jrcqd**.